Pressure Drop and Vortex Size of Power Law Fluids Flow in Branching Channels with Sudden Expansion

H. Ameur[†]

Department of Technology, Institute of Science and Technology, University Center Ahmed Salhi of Naâma (Ctr Univ Naâma), PO. 66, 45000, Algeria

† *Email: houari_ameur@yahoo.fr; h.ameur@mail.cuniv-naama.dz*

ABSTRACT

Three dimensional flows of complex non-Newtonian fluids in sudden expending pipes are numerically investigated in this paper. The distribution channels have one or multiple inlet pipes and one outlet pipe. The working fluids have a shear thinning behavior modeled by the Ostwald De Waele law. The effects of different parameters on the flow fields and pressure drop are explored. It concerns the effect of Reynolds number Re (from 0.1 to 600), power law index n (from 0.4 to 1), number of branching channels (n_b = 1, 2, 3 and 4), spacing between the branching channels (l/D = 0.1, 0.2, 0.3 and 0.4) and the expansion ratio (d/D = 0.2, 0.35, 0.5, 0.6 and 0.8). Three-dimensional complex flows were observed in the downstream expansion for such multiple branching systems, especially when the spacing l/D is small, where an asymmetry of flows is observed and a third recirculation loop is formed. A considerable increase in pressure drop is found with the rise of Reynolds number, with increased power law index and decreased expansion ratio. However, only a slight increase is observed with decreased spacing ratio and it remained almost the same with increased number of branching channels.

Keywords: Branching channels; Sudden expansion; Shear thinning fluids; Pressure drop; Vortex.

1. INTRODUCTION

The flows of bio-medical, chemical and other industrial fluids in ducts and pipelines are highly encountered in industrial machines. The distribution of these liquids from a position to another is achieved for various objectives, such as in air conditioning systems, heat exchangers, pulmonary and cardiovascular flow systems, hydraulic controls, etc. In delivering systems, the pipes are usually connected at junctions with sudden expansion or contraction for network distribution (Joseph and Allen, 1996). The sudden abrupt geometrical expansions have been also used as a model of flow in arterial stenoses in biomedical applications (Peterson and Plesniak, 2008; Vétel *et al*., 2008 ; Griffith *et al*., 2008; Mao *et al*., 2011; Casas *et al*., 2016; Petersson *et al*., 2016).

he flows through a symmetric pipe deflect to one side along the longitudinal direction (i.e. the symmetric axis of pipe) (Yamaguchi *et al*., 2006). This deflection is characterized by the flow rate ratio cross outlet branch pipes, and it is generally considered as an instability problem of flow described by the bifurcation theorem (Mizushima and Shiotani, 2000).

Many experimental studies revealed the presence of oscillations and unsteadiness of flows in pipes with sudden expansion. But, there is no agreement concerning the value of Reynolds number at which the unsteadiness occurs and the main reason of this discrepancy is the effect of the inlet profile (Cantwell *et al*., 2010). Drikakis (1997) investigated by numerical computations the effects of expansion ratio on the planar expansion flows of Newtonian fluids. They found a reduction of the critical Reynolds number for the symmetry-breaking bifurcation with the increase of the expansion ratio. Mullin *et al*. (2009) pointed out in their experimental study on the Newtonian fluid flow through a 1:2 expanding-pipe that the steady-state breaking of axisymmetry occurs at Re = 1139 ± 10. This symmetry breaking of flow is the rotational analog of that remarked in the symmetric planar expansion (Drikakis, 1997). For a Newtonian fluid, Battaglia and Papadopoulos (2006) explored the 3D influence on the bifurcation characteristics at low Reynolds number (from 150 to 600) flows in rectangular sudden expansions. Praveen and Eswaran (2017) predicted the bifurcation characteristics of an incompressible Newtonian fluid in a 2-D symmetric sudden expansion at low Reynolds number (smaller than 100). They

determined the critical Reynolds number by using a temporal measure of asymmetry which is found to be more efficient than the existing steady-state techniques. They reported that the streamwise magnetic field delay the flow transition to asymmetry situation.

The reattachment length decreases with the rise of swirling flows in abrupt expanding pipes (Vanierschot and Van den Bulck, 2008). Cantwell et al. (2010) performed a numerical investigation of the transient growth experienced by infinitesimal perturbations to a Newtonian fluid flow through a circular pipe with 1:2 sudden expansions. Under steady state laminar conditions, they determined the downstream reattachment point vs. Reynolds number and they reported that the flow is linearly stable at least up to $Re = 1400$.

Kaushik et al. (2012) explored by CFD method the core annular flow of water and lubricating oil in a sudden contraction and expansion. Liou and Lin (2014) conducted numerical computations of the pressure-driven rarefied gas flow in channels with a sudden contraction–expansion of 2:1:2. Paik and Sotiropoulos (2010) explored numerically the turbulent swirling flow of a Newtonian fluid in a sudden expansion.

In fact, the fluids encountered through flow devices have a complex non-Newtonian behavior in many realistic situations. Therefore, it is relevant to assess the effect of specific rheological features upon the flow details in branching channels with abrupt expansion. If the concentration of non-Newtonian liquids is low, the Reynolds numbers tend to be high and may be lead to turbulent regime.

Interested to the viscous fluids described by Casson and power-law models and flowing through a 1:2 planar sudden expansion, Neofytou (2006) studied the effect of Reynolds number and the flow behavior index (n ranging from 0.3 to 3) on the hydrodynamic behavior and they explored the transition from symmetric to asymmetric flow. Using CFD simulations, Manica and De Bortoli (2004) investigated the flow characteristics of shear-thinning and shear thickening fluids ($n = 0.5, 1$ and 1.5) through a 1:3 planar sudden expansion. For a Reynolds number ranging between 30 and 125, their results revealed that the critical Reynolds number for the flow bifurcation of Newtonian fluids is lower than that for shear-thinning fluids, and that for shear-thickening fluids is the lowest. By experiments and numerical simulations, Mishra and Jayaraman (2002) explored the asymmetric steady flow of shear-thinning fluids in planar sudden expansions having a wide expansion ratio (ER = 16).

By using CFD simulations, Pinho et al. (2003) interested to inelastic shear thinning fluids through abrupt expansions channels with a diameter ratio varying from 1 to 2.6. When changing the flow behavior index from 1 to 0.2, they found an increase in local friction coefficient by about 100% at low Reynolds number and an increase by more than 50% at high Re. For a 1:3 planar symmetric expansion, Ternik et al. (2006) compared the results of power-law and quadratic viscosity models for shear-thickening fluids with those of Newtonian liquids and they showed the great impact of the shear-thickening behavior on the flow asymmetry. For a 1:3 planar sudden expansion and by using computational method, Ternik (2009), studied the flow of shear-thinning fluids with two values of flow behavior index $n = 0.6$ and 0.8. They reported that from a symmetric to asymmetric flow and after the first bifurcation, a second flow bifurcation marking the appearance of a third vortex occurs with the rise of Reynolds number. In another paper and by numerical simulations, Ternik (2010) studied the flows of shear thinning fluids with a power index varying between 0.6 and 1.4 through a 1:3 sudden expansion. They focused here on the low Reynolds number flow (in the range of Re between 10^{-4} and 10). For a 1:3 planar sudden expansion, Dhinakaran et al. (2013) studied numerically the flow of power law fluids with power-law indices varying in the range from 0.2 to 4 and Reynolds number between 0.01 and 600. They determined the values of the critical Reynolds number for the transition to asymmetry flow and the appearance of a third main vortex. They pointed out a decrease in the critical Re with the shear thickening behavior, and an opposite influence of the shear thinning behavior. Small recirculation regions, typical of creeping flow are formed for shear-thinning fluids, resulting thus in a reduction of intensity and size of the secondary flow.

For a polymer melt modeled by the cross constitutive relation, Zdanski and Vaz Jr (2009) studied numerically the non-isothermal flow through abrupt expansions and they observed a complex 3D flow structures characterized by a spiral motion close to the expansion section. They found also a limited effect caused by the viscous dissipation on the temperature increase and changes in viscosity which is strongly affected by the shear rate. Mendes et al. (2007) explored numerically and by experiments the viscoplastic fluid flow through a sudden expansion followed by a sudden contraction. They found a strong dependence of the size of the unyielded zone upon the rheological and geometrical parameters. This unyielded zone is positioned in the section of channel with wide diameter close to the wall. Naccache and Barbosa (2007) studied the creeping flow of viscoelastic fluids in a planar expansion followed by a contraction. Poole et al. (2007) studied numerically the creeping flow of viscoelastic fluids in a 1:3 planar abrupt expansion and they found a reduction in the length and intensity of the recirculation region downstream of the expansion caused by the fluid elasticity. They observed also the existence of a significant recirculation zone for these fluids even at high Deborah number. For Newtonian fluids, it is known that the asymmetric flows in abrupt expansion pipes appear at a diameter ratio greater than 1.5. However and for the viscoelastic fluids, this asymmetry has been found by Poole and Escudier (2003) to be reduced initially at ($x/d < 6$) but not eliminated and the flow remain three-dimensional and highly complex.

Concerning the branching channels, there are only

few papers available in the literature. Liepsch (2002) studied the case of branching geometry in vascular flows. Yamaguchi *et al.* (2006) studied numerically and by experiments the deflection characteristics of Newtonian fluid flows in a manifold distribution channel with one inlet and two outlet pipes. Their results revealed a large dependency of the defection characteristics upon the net contribution of the swirl component in the expanded pipe part before entering each delivering outlet channel. In another study (Yamaguchi *et al.*, 2005) for an incompressible Newtonian fluid, they observed the existence of two distinct domains of strong asymmetric flow distribution from the outlet branch channels, which are dependent upon Reynolds numbers. They observed also a time periodicity of flow with the rise of Reynolds number.

For complex non-Newtonian fluids and especially for power-law fluids, different pictures of the occurrence of flows of such fluids in branching channels may be encountered in many processes (in medical, cosmetic, paint industries, etc.) such as the flow of blood in vascular, the flow of paint mixture and other cases.

Our search in literature showed that there is no published paper regarding the flows in branching channels with complex fluids. View their great importance in fluid engineering and in practical uses, we explore here the characteristics of shear thinning fluid flows through a cylindrical distribution channel with one or multiple inlet pipes and one outlet pipe. The connecting section is characterized by an abrupt expansion. Effects of the following parameters on the flow fields and pressure drop are examined: the number of branching channels (n_b = 1, 2, 3 and 4), spacing between the branching channels (l/D = 0.1, 0.2, 0.3 and 0.4) and the expansion ratio (d/D = 0.2, 0.35, 0.5, 0.6 and 0.8), Reynolds number *Re* (from 0.1 to 600) and rheological properties of fluids (power law index *n* is varied from 0.4 to 1). Such an effort is expected to provide a physical insight into the phenomenon for a wide range of geometric, physical and operating parameters.

2. PRESENTATION OF THE PROBLEM

Geometry of the problem studied is shown in Fig. 1. It concerns a cylindrical pipe with abrupt expansion. In the upstream region of abrupt expansion, there is a pipe of sufficient length L_1 and diameter *d* to ensure the fully developed inlet flow. L_1 is taken equal to 30 times the diameter *d* and it not changes with Reynolds number. This value was taken by many authors for studying the flows through pipes. Also, in the downstream region of the abrupt expansion, there is a pipe sufficiently long (length L_2, diameter *D*) to permit the reattachment and fully redevelopment of flow again. Inelastic shear thinning fluids are used as working fluids. Effects of power law index (*n*) are examined (*n* = 0.4, 0.6, 0.8 and 1).

Also, effects of the diameter ratio (*d/D*), number (n_b) of branching channels (Fig. 2) and spacing between them (*l/D*) are investigated. The required details on all realized geometrical configurations are summarized in Table 1.
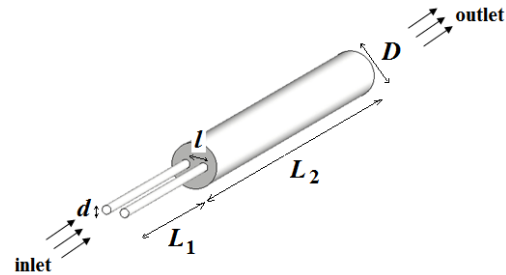

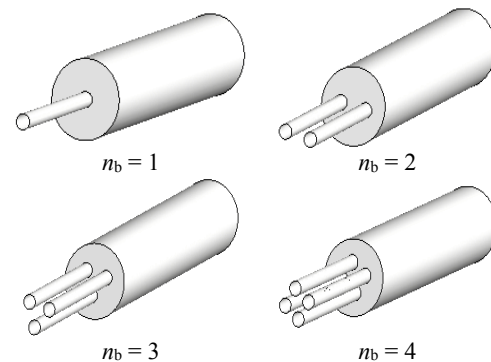**Fig. 1. An example of sudden expanded piping systems studied**

Fig. 2. Schematic view of sudden expanded piping systems with different numbers (n_b) of branching channels

Table 1. Geometrical parameters of all cases studied

d/D	l/D	n_b
0.2	0.2	1
		2
		3
		4
0.2	0.1	2
	0.2	
	0.3	
	0.4	
0.2	0	1
0.35		
0.5		
0.65		
0.8		

3. MATHEMATICAL FORMULATION

The three-dimensional flows of complex fluids were simulated by using the computer code CFX 16.0. For an incompressible and isothermal flow, and a purely viscous shear thinning fluid, the equations of continuity (Eq. (1)) and momentum (Eq. (2)) are given by:

$$\frac{\partial u_i}{\partial x_i} = 0 \tag{1}$$

$$\rho\left[\frac{\partial\left(u_i u_j\right)}{\partial x_j}\right]=-\frac{\partial p}{\partial x_i}+\frac{\partial}{\partial x_j}\left[\eta\left(\dot{\gamma}\right)\left(\frac{\partial u_i}{\partial x_j}+\frac{\partial u_j}{\partial x_i}\right)\right] \qquad (2)$$

where ρ is the fluid density, p is the pressure, $\dot{\gamma}$ is the shear rate and η is the apparent viscosity given by:

$$\eta\left(\dot{\gamma}\right)=k\,\dot{\gamma}^{n-1} \qquad (3)$$

where n is the power index and k is the consistency index of the Ostwald de Waele power law.

The shear rate $\dot{\gamma}$ is related to the second invariant of the deformation rate tensor (D_{ij}) as:

$$\dot{\gamma}=\sqrt{2D_{ij}D_{ij}}\ \text{ with }D_{ij}=\frac{1}{2}\left(\frac{\partial u_i}{\partial x_j}+\frac{\partial u_j}{\partial x_i}\right) \qquad (4)$$

The friction factor (f) is calculated using the following equation (Pinho *et al*., 2003):

$$f=\frac{4\tau_w}{\frac{1}{2}\rho V_{in}^2}\frac{d}{2r} \qquad (5)$$

where r is the radial coordinate, τ_w is the wall shear stress. The Reynolds number (Re) for a circular pipe is given by:

$$Re=\frac{\rho V_{in}d}{\mu_a} \qquad (6)$$

where μ_a is the apparent viscosity. For the power law fluids studied here, we used the generalized Reynolds number given by Metzner and Reed (1955), which is defined in terms of upstream channel characteristics:

$$Re_g=\frac{\rho V_{in}^{2-n}d^n}{k}8\left(\frac{n}{6n+2}\right)^n \qquad (7)$$

The diameter (d) and the velocity (V_{in}) at the inlet pipe are used to write the dimensionless form of coordinates and velocity (Eq. (8)).

$$X^*=\frac{X}{d}\ ;V^*=\frac{V}{V_{in}} \qquad (8)$$

where $V = (u, v, w)$ is the velocity vector and $X = (x, r, \theta)$ is the coordinate.

The friction coefficient on the wall permits to determine the point of reattachment flow. It is defined as:

$$C_f\left(x\right)=\frac{2}{Re}\left(\frac{\partial u}{\partial y}\right)_{wall} \qquad (9)$$

4. NUMERICAL DETAILS

The geometry and mesh are created by the computer tool ANSYS ICEM CFD (version 16.0). The computational domain was discretized by tetrahedral mesh elements (Fig. 3). A refined mesh near the walls and the abrupt section was created in order to capture the flow details. Grid dependency was performed by changing the number of elements from 100,000 to 1,300,000. From a grid with 1,212,564 elements, the velocity with high magnitude, the reattachment length and the deflection rate did not change by more than 2%. Therefore, this number was selected to achieve all computations. The second order central difference scheme was used to approximate the diffusion term in the momentum and energy equations. This scheme is known by its stable solution. For the discretization of convection terms, a second-order upwind scheme was used. The Navier-Stockes governing equations were solved by a segregated implicit iterative scheme.

The SIMPLE (Semi-Implicit Pressure Linked Equation) algorithm was used to deal with the pressure–velocity coupling (Issa and Oliveira, 1994). Conjugate gradient methods were employed to solve the linear equations (preconditioned bi-conjugate solver for u and v, symmetric conjugate solver for p).

Boundary conditions of the computational domain are as follows:

- Before the entrance of the sudden expanded section, the flow is assumed to be fully developed, since the length L_1 is sufficient ($L_1 = 30*d$). The Dirichlet conditions in this case are: $u^* = V_{in}, v^* = 0, w^* = 0$

- At the exit of pipe, the flow is considered as fully developed and the following Neumann condition is defined ($\partial V^*/\partial x^* = 0$). Also, a pressure outlet boundary condition (set to zero) was used in the numerical scheme.

- At every wall of the computational domain, the non-slip flow condition is given by the following Dirichlet conditions: $u^* = 0, v^* = 0, w^* = 0$

Many researchers studied numerically the power law-fluids flows through abrupt expended pipes by using open source or commercial computer codes. The convergence of solution was found to be a major limitation with small or great values of flow behavior index (n). For example, Pool and Ridley (2007) did not obtained converged solution with a flow behavior index smaller than 0.4. With the OpenFOAM code, Ternik (2009) found a continue increase in the number of iterations and computational time with the decrease of the flow behavior index and no convergence has been obtained for n smaller than 0.6. In this paper, values of n are varied from 0.4 to 1 and no problem of convergence has been encountered for this range when using the computer code CFX. However, the computational time and iterative convergence has been raised with the reduction of n.

The residual target for the continuity, momentum and energy equations was 10^{-7}. Most simulations required about 500-900 iterations and about 2-3 h on a computer machine with Intel Core i7 CPU, 8.0 GB of RAM and a clock speed of 2.20 GHz.
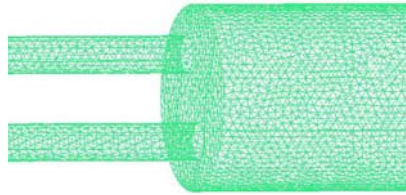
Fig. 3. Discretized of the computational domain with tetrahedral mesh elements.

5. VALIDATION OF THE PREDICTED RESULTS

Mesh resolutions, machine limitations, computer code and numerical method accuracy may cause severe errors in predictions. Therefore, it is strongly required to check the validity of the obtained results. In our study, we referred to several studies dealing with inelastic power law fluids.

First, the geometrical and rheological conditions as those chosen by Kahine *et al.* (1997) were undertaken. Variations of the axial velocity for a power law index $n = 0.6$ and an expansion ratio $d/D = 0.112$ vs. axial distance (X^*) are presented on Fig. 4. Both our predicted results and the experimental data of Kahine and his co-worker follow the same profile with a satisfactory agreement.

In other figures, we present the vortex length (Fig. 5) and vortex height (Fig. 6) for different power law indices. The results predicted by our computer code and those calculated by the correlations of Dhinakaran *et al.* (2013) and Ternik (2010) are depicted on the same figures for sake of comparison. The developed correlations are:

$$\frac{X_a}{d} = 0.382 + 0.414 \tanh\left(1.142\,n - 0.775\right)$$

(Dhinakaran *et al.*, 2013)

$$\frac{X_a}{d} = -0.1463\,n^2 + 0.6702\,n + 0.0035$$

(Ternik, 2010)

$$\frac{Y_a}{d} = 1.03 + 0.49 \tanh\left(-1.72\,n + 1.13\right)$$

(Dhinakaran *et al.*, 2013)

$$\frac{Y_a}{d} = -0.449\,n^2 - 1.5058\,n + 1.8345$$

(Ternik, 2010)

In another framework, we present the friction factor at the inlet pipe vs. generalized Reynolds number (Fig. 7). Our numerical results by using Eq. (5) and those obtained by theoretically ($f = 64/Re_g$) are showed on the same figure. As observed on these figures, a good agreement qualifies the performance of the utilized computer tool.
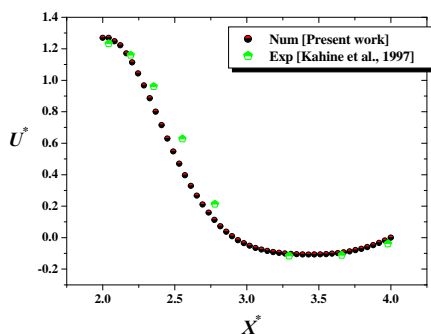

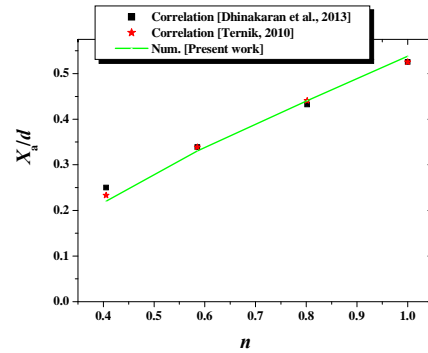**Fig. 4. Axial velocity for $n = 0.6$, $d/D = 0.112$**
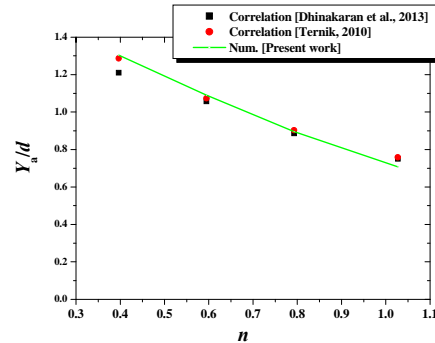

Fig. 5. Vortex length vs. power law index.
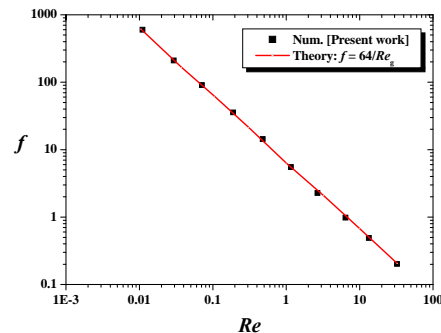

Fig. 6. Vortex height vs. power law index.

Fig. 7. Friction factor at the inlet pipe vs. Reynolds number.

6. RESULTS AND DISCUSSION

Understanding the flows in abrupt expansion pipes is of a keen interest from the view-point of practical uses. These devices have a widespread presence in various applications of fluid mechanics such as in combustors, heat exchangers, nuclear reactors as well as in biological systems. The flow in an axisymmetric abrupt expansion is three-dimensional and complex and characterized by the presence of separating and reattaching flows.

6.1 Effect of Reynolds Number

In this section, we examine the effect of flow rate, by changing the Reynolds number from 0.1 up to order 600. Figure 8a presents the dimensionless axial velocity along the pipe radius for different values of Reynolds number, in the downstream of the expansion section at $X^* = 27.5$. Velocities with high magnitude are located at the centerline of each inlet pipe (here $n_b = 2$), and negative velocities are observed near the wall of channel, which indicate the presence of opposite flow. Figure 8b shows the

profiles of dimensionless axial velocity near the channel wall in the downstream of expansion. As observed, the intensity of opposite flow increases with increased Reynolds number. The size of recirculation loops and their strength increase with the rise of flow rate, as confirmed by the streamlines of Fig. 9. These vortices are characterized by high pressure gradients and strong shear stresses (τ^*), which increase with increased Reynolds number, as illustrated by Fig. 10 where values of τ^* near the pipe wall and past the expansion are presented.

(a) $X^* = 27.5$

(b) $R^* = 0.99$
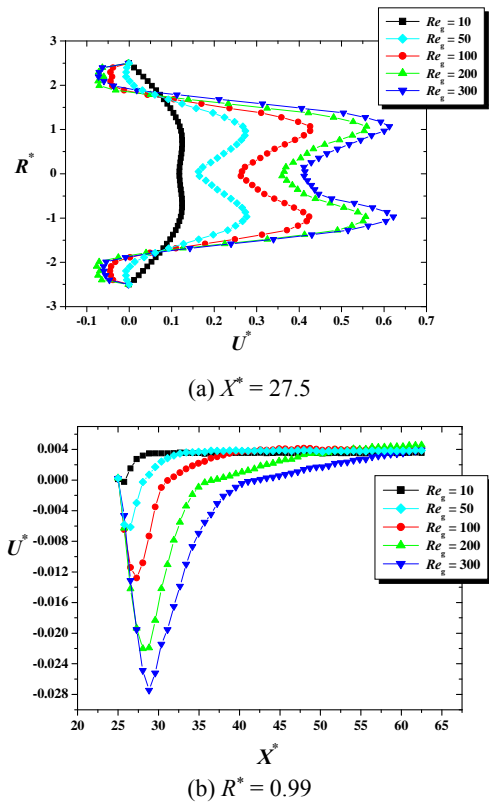
Fig. 8. Axial velocity for $n = 0.75$, $n_b = 2$, $d/D = 0.2$, $l/D = 0.2$
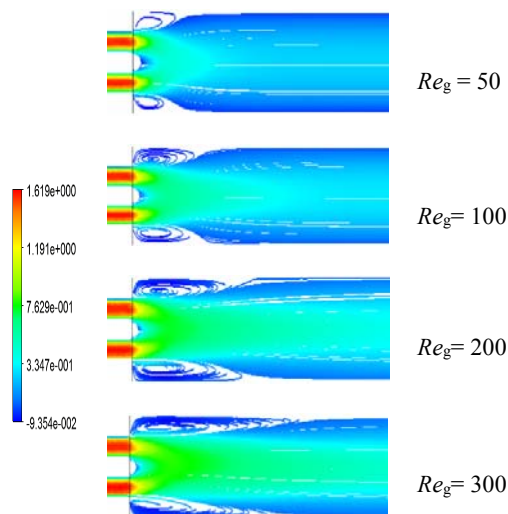
Fig. 9. Streamlines of the dimensionless axial velocity U^* for $n = 0.75$, $n_b = 2$, $d/D = 0.2$, $l/D = 0.2$
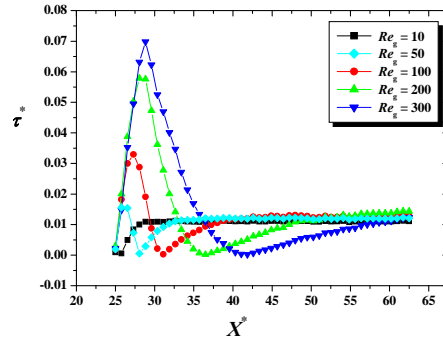
Fig. 10. Shear tress for $n = 0.75$, $n_b = 2$, $d/D = 0.2$, $l/D = 0.2$, $R^* = 0.99$

6.2   Effect of the flow behavior index

Another validation of our predicted results is available in Fig. 11, where the dimensionless recirculation length is presented for various Reynolds numbers. As shown on this figure, our results agree well with the experimental data of Ponthieu (1991) and the numerical results of Nguyen *et al.* (1999).

Both numerical (Hammad *et al.*, 1999; Furuichi *et al.*, 2003; Mullin *et al.*, 2009) and experimental (Badekas and Knight, 1992) works pointed out that there is a linear change in the reattachment length vs. Reynolds number in the steady state, with a dependence proportionality on whether the profile of inlet flow is fully developed Hagen–Poiseuille or flat (Cantwell *et al.*, 2010). The finding provided in Fig. 12 confirms the linear increase of recirculation length vs. Reynolds number, which is also raised with the increase in power law index. The strength of vortices and their size decrease with the raise of shear thinning, which is due to the increased local viscosity caused by low shear rates inside these vortices.

This phenomenon may be also explained by the velocity profiles plotted on Fig. 13 at $X^* = 27.5$ (i.e. in the downstream expansion). With increased power law index, high viscous forces characterize the powerful jet of fluid (in the center of redeveloping flow downstream the expansion) and in the zone of recirculation. The increase of viscosity inside these eddies is also responsible for the increase in pressure drop (Fig. 14).
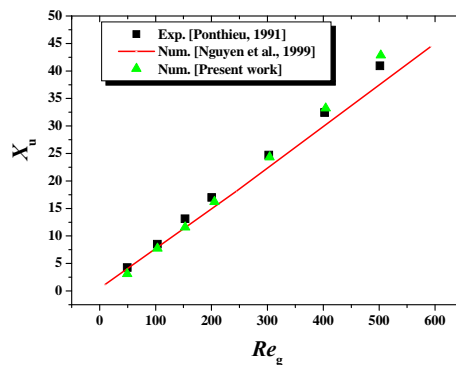

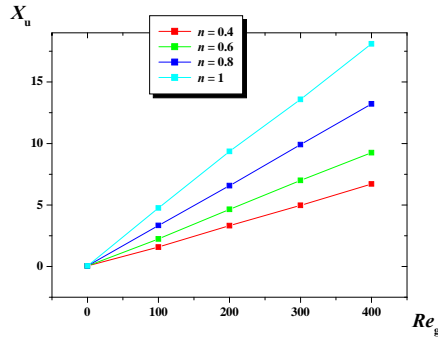**Fig. 11. Reattachment length for $n = 0.5$, $d/D = 0.112$, $n_b = 1$**

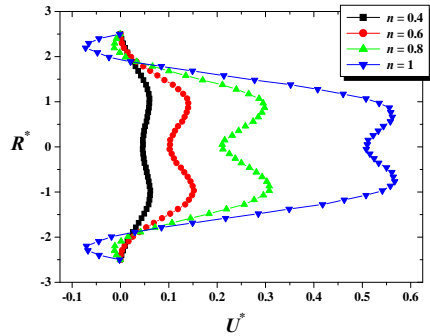**Fig. 12. Reattachment length for $d/D = 0.35$, $n_b = 1$**

Fig. 13. Axial velocity for $Re_g = 50$, $n_b = 4$, $d/D = 0.2$, $X^* = 27.5$
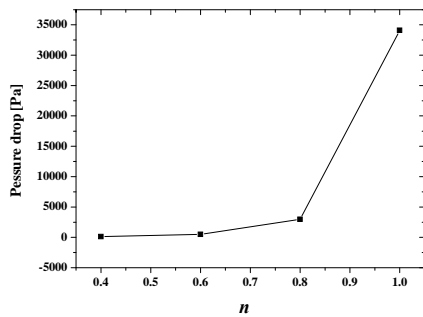

Fig. 14. Pressure drop for $Re_g = 50$, $n_b = 4$, $d/D = 0.2$, $X^* = 27.5$

6.3   Effect of the Distance *L*

When a viscous fluid flowing in a pipe encounters an abrupt expansion, the separation of flow occurs, resulting thus in the formation of a pair of symmetric recirculation loops near the downstream walls. This symmetry will be loosed above a critical value of Reynolds number, and a third eddy will appear downstream of the two main eddies with the further rise of *Re*. The transition of flow from symmetric to asymmetric situation, which is known as bifurcation phenomenon, depends on the geometrical parameters of channel and rheological properties of fluid. In this part of paper, we investigate the effect of the space ratio (l/D) between branching channels by realizing four geometries, which are: $l/D = 0.1$, 0.2, 0.3 and 0.4.

For the four geometries having the same diameter ratio $d/D = 0.2$, the recirculation size and its strength are clearly illustrated in Fig. 15 on two different planes (*XY* plane on left and *XZ* plane on right). When the spacing l/D between the two branching channels is very low ($l/D = 0.1$), an asymmetry of recirculation loops happens and three-dimensional complex flows are formed in the downstream region of expanding system. In this case, the interaction between fluid particles is very strong, leading to the formation of third recirculation loop before the reattachment of the main flow.

This asymmetry in flow will be loosed with the increased spacing ratio (for $l/D = 0.2$), which allows less interaction between the jet flows at the exit of branching channels. Also, the further rise in l/D reduces the length of vortex and increases their height. Furthermore, when the spacing l/D is increased again ($l/D = 0.4$), fair vortices are present at the exit region of branching pipes and very small eddies at the corner of expansion.

For further explanation, we present on Fig. 16 the dimensionless axial velocity along the pipe radius at $X^* = 27.5$ (i.e. near the downstream expansion). The increase of l/D yields weak flows in the region between the exit of branching channels and intensifies the fluid movement near the channel walls, which eliminates the vortices in the corners
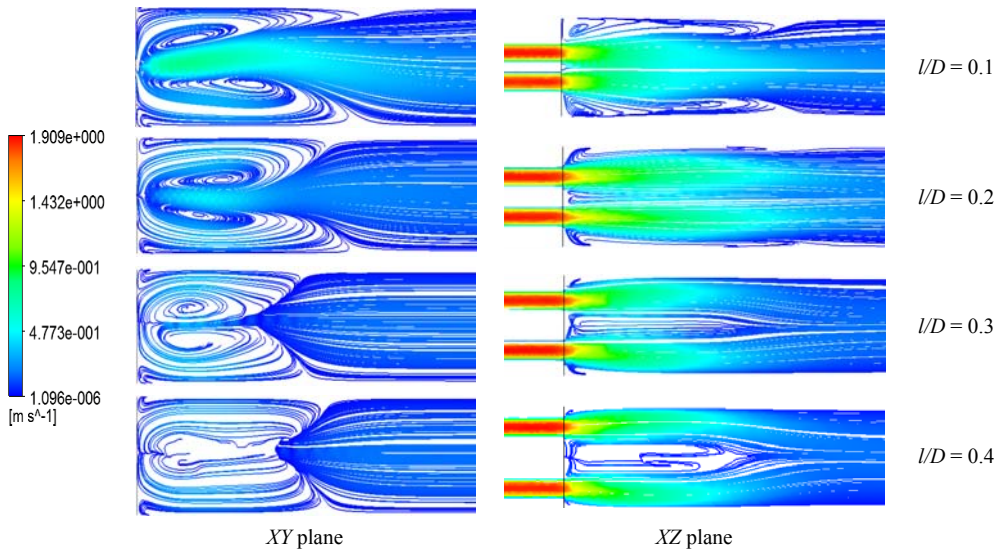

Fig. 15. Streamlines for $Re_g = 200$, $n = 0.75$, $n_b = 2$, $d/D = 0.2$

of expansion. On the other hand, the pressure drop increases considerably with the rise of Reynolds number and only slight increase is observed with the rise of spacing ratio (Fig. 17).

6.4 Effect of n_b

In this section, we explore the influence of the number (n_b) of branching channels. Four cases are considered, n_b = 1, 2, 3 and 4 with an expansion ratio d/D = 0.2 of each branching channel.

Distribution of the axial velocity is presented under different forms: contours on Fig. 18 and streamlines on Fig. 19. As shown on Figs. 18 and 20a, the increase of the number of branching channels yields a powerful jet of fluid, resulting thus in further interaction of fluid particles in the downstream expansion. The height of vortex becomes smaller (Fig. 20b), but the reattachment length increases with increased n_b, as observed on Fig. 19.

The pressure losses are calculated for the four geometrical cases and presented on Fig. 21. The interesting finding is that the different in pressure drop between the cases studied is very slight. The flow rate increases with the increasing number of branching channels, so the different in pressure drop between the inlet and outlet sections of the device remains almost the same for all geometrical configurations. This finding confirms that the main responsible parameter in energy losses in such channel configurations is the sudden expansion in diameter.
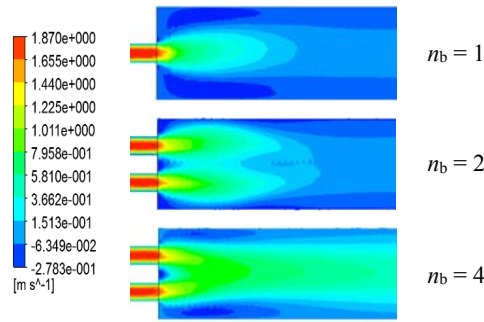

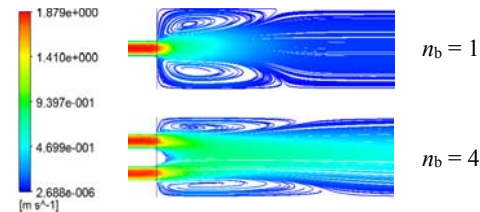**Fig. 18. Axial velocity for Re_g = 200, n = 0.75, d/D = 0.2**
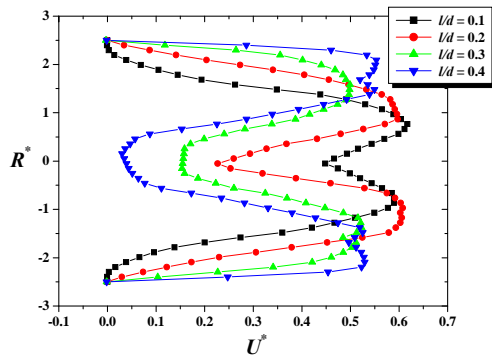

Fig. 19. Streamlines for Re_g = 200, n = 0.75, d/D = 0.2

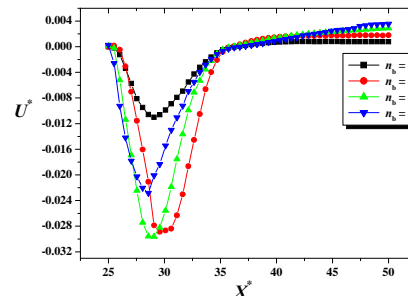(a) X^* = 27.5

(b) R^* = 0.99

Fig. 20. Axial velocity for Re_g = 200, n = 0.75, d/D = 0.2

Fig. 16. Axial velocity for Re_g = 200, n = 0.75, n_b = 2, d/D = 0.2, X^* = 27.5
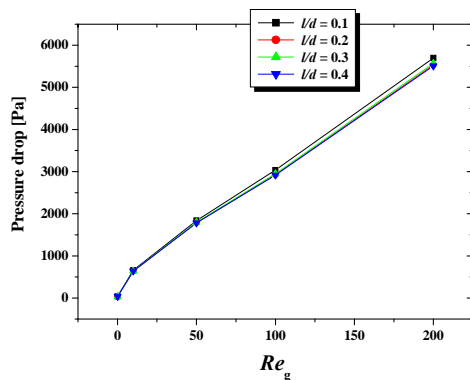

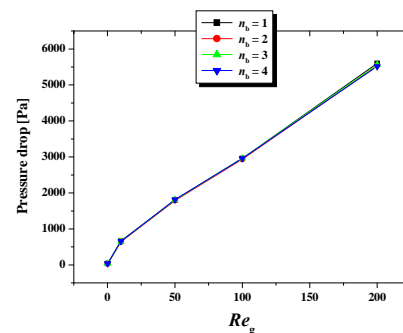**Fig. 17. Pressure drop for n = 0.75, n_b = 2, d/D = 0.2**

Fig. 21. Pressure drop for n = 0.75, d/D = 0.2

6.5 Effect of *d/D*

The effect of expansion ratio (*d/D*) is examined in this section. Five geometrical configurations are realized to achieve this purpose, which are: *d/D* = 0.2, 0.35, 0.5 and 0.65. For one branching channel (n_b = 1) and a shear thinning fluid with a power law index *n* = 0.75 and flow Reynolds number Re_g = 200, the velocity streamlines are presented on Fig. 22 for four geometries on horizontal plane *XY*. This figure allows a clear visualization of recirculation loops developed downstream the expansion, which decrease in size and strength with the increase of expansion ratio. For further details, values of the reattachment length corresponding to each geometrical configuration are given on Fig. 23 for different power law indices. The decrease in power law index yields a decrease of reattachment length. However, the expansion ratio has an opposite effect, which results in increasing pressure drop as observed on Fig. 24. The interesting remark is that the discrepancy in pressure drop between the five geometrical cases becomes greater with the rise of Reynolds number. For instance, at Re_g = 200, the pressure drop has been increased by about 14 times, 4 times, 1.8 and 1.2 times for the expansion ratio *d/D* = 0.2, 0.35, 0.5 and 0.5, respectively, when compared to the case *d/D* = 0.8.
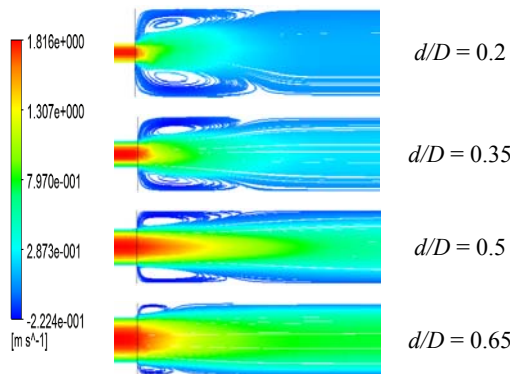

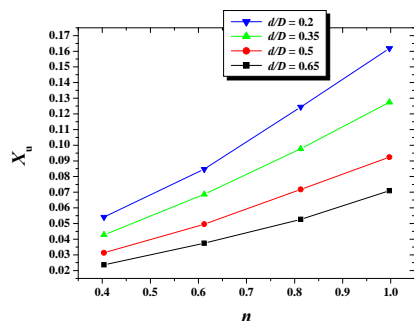**Fig. 22. Streamlines for *n* = 0.75, n_b = 1, Re_g = 200, α = 90°**

Fig. 23. Reattachment length for *Re* = 100, n_b =1

7. CONCLUSION

Three-dimensional flows of power law fluids through branching channels with sudden expansion were numerically investigated. Velocity distribution, vortex size, reattachment length and
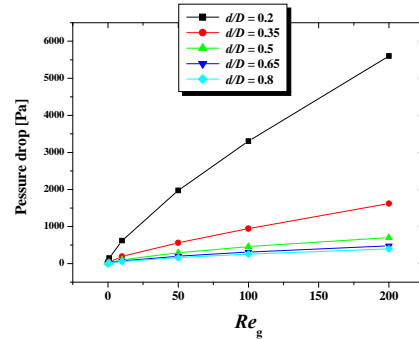

Fig. 24. Pressure drop for *n* = 0.75, n_b = 1

pressure drop were determined for various operating conditions. After the expansion section, a longer axial distance was considered aiming to capture the entire redevelopment of flow after reattachment. Effect of Reynolds number, shear thinning behavior, expansion ratio, number of branching channels and spacing between them were assessed. The main findings are summarized as follows:

- The shear thinning reduced the recirculation length and weakened the strength of eddies.

- The pressure drop is increased with the rise of Reynolds number and power law index.

- A third vortex is observed near the downstream expansion when the spacing ratio *l/D* is very small.

- The increase of spacing ratio *l/D* weakened the intensity of flows in the region between the exit of branching channels and intensified the movement of fluid particles near the channel walls.

- The excessive increase of spacing ratio *l/D* eliminated the vortices in the corners of expansion.

- The vortex size rose with the increased Reynolds number and decreased expansion ratio

- A considerable increase in pressure drop is found with decreased expansion ratio. However, only a slight increase in observed with decreased spacing ratio and it remained almost the same with increased number of branching channels.

REFERENCES

Badekas, D. and D. D. Knight (1992). Eddy correlations for laminar axisymmetric sudden expansion flows. *ASME Journal of Fluids in Engineering* 114, 119–121.

Battaglia, F. and G. Papadopoulos (2006). Bifurcation characteristics of flows in rectangular sudden expansion channels. *Journal of Fluids Engineering* 128, 671–679.

Cantwell, C. D., D. Barkley and H. M. Blackburn, (2010). Transient growth analysis of flow through a sudden expansion in a circular pipe. *Physics of Fluids* 22, 034101.

Casas, B., J. Lantz, P. Dyverfeldt and T. Ebbers (2016). 4D flow MRI-based pressure loss

estimation in stenotic flows: evaluation using numerical simulations. *Mag. Res. Med.* 75, 1808–1821.

Dhinakaran, S., M. S. N. Oliveira, F. T. Pinho and M. A. Alves (2013). Steady flow of power-law fluids in a 1:3 planar sudden expansion. *Journal of Non-Newtonian Fluid Mechanics* 198, 48–58.

Drikakis, D. (1997). Bifurcation phenomenon in incompressible sudden expansion flows. *Physics of Fluids* 9, 76–87.

Furuichi, N., Y. Takeda and M. Kumada (2003). Spatial structure of the flow through an axisymmetric sudden expansion. *Experiments in Fluids* 34, 643–650.

Griffith, M. D., T. Leweke, M. C. Thompson and K. Hourigan (2008). Steady inlet flow in stenotic geometries: Convective and absolute instabilities. *Journal of Fluid Mechanics* 616, 111-133.

Hammad, K. J., M. V. Otugen and E. B. Arik, (1999). A PIV study of the laminar axisymmetric sudden expansion flow. *Experiments in Fluids* 26, 266–272.

Issa, R. and P. J. Oliveira (1994). Numerical prediction of phase separation in two-phase flow through T-junctions. *Computers and Fluids* 23, 347–372.

Joseph, A. S. and E. F. Allen (Eds.), Handbook of Fluid Dynamics and Fluid Machinery 3, Wiley, 1996, pp. 2005–2018.

Kahine, K., V. T. Nguyen and M. Lebouché (1997). Flow of non-Newtonian fluids in sudden expansions. *International Communications in Heat and Mass Transfer* 24, 1103–1112. (In French)

Kaushik, V. V. R., S. Ghosh, G. Das and P. K. Das (2012). CFD simulation of core annular flow through sudden contraction and expansion. *Journal of Petroleum Science and Engineering* 86–87, 153–164.

Liepsch, D. (2002). An introduction to biofluid mechanics – basic models and applications. *Journal of Biomechanics* 35, 415–435.

Liou, T. M. and C. T. Lin (2014). Study on microchannel flows with a sudden contraction–expansion at a wide range of Knudsen number using lattice Boltzmann method. *Microfluidics Nanofluidics* 16, 315–327.

Manica, R. and A. L. De Bortoli (2004). Simulation of sudden expansion flows for power-law fluids. *Journal of Non-Newtonian Fluid Mechanics* 121, 35–40.

Mao, X., S. J. Sherwin and H. M. Blackburn (2011). Transient growth and bypass transition in stenotic flow with a physiological waveform. *Theoretical and Computational Fluid Dynamics* 25, 31–42.

Mendes, P. R. S., M. F. Naccache, P. R. Varges and F. H. Marchesini (2007). Flow of viscoplastic liquids through axisymmetric expansions–contractions. *Journal of Non-Newtonian Fluid Mechanics* 142, 207–217.

Metzner, A. B. and J. C. Reed (1955). Flow of non-Newtonian fluids - correlation of the laminar, transition and turbulent flow regimes. *AIChE Journal* 1, 434–440.

Mishra, S. and K. Jayaraman (2002). Asymmetric flows in planar symmetric channels with large expansion ratio. *International Journal of Numerical Methods in Fluids* 38, 945–962.

Mizushima, J. and Y. Shiotani (2000). Structural instability of the bifurcation diagram for two-dimensional flow in a channel with a sudden expansion. *Journal of Fluid Mechanics* 420, 131–145.

Mullin, T., Seddon, J. R. T., Mantle, M. D. and Sederman, A. J. (2009). Bifurcation phenomena in the flow through a sudden expansion in a circular pipe. *Physics of Fluids* 21, 014110.

Naccache, M. F. and R. S. Barbosa (2007). Creeping flow of viscoplastic materials through a planar expansion followed by a contraction. *Mechanics Research Communications* 34, 423–431.

Neofytou, P. (2006). Transition to asymmetry of generalised Newtonian fluid flows through a symmetric sudden expansion. *Journal of Non-Newtonian Fluid Mechanics* 133, 132–140.

Nguyen, V. T., K. Kahine and M. Lebouché (1999). Numerical study of non-Newtonian fluid flows through sudden expansions. *Compte Rendu de l'Académie des Sciences* 327, 91–94.

Paik, J. and F. Sotiropoulos (2010). Numerical simulation of strongly swirling turbulent flows through an abrupt expansion. *International Journal of Heat and Fluid Flow* 31, 390–400.

Peterson, S. D. and M. W. Plesniak (2008). The influence of inlet velocity profile and secondary flow on pulsatile flow in a model artery with stenosis. *Journal of Fluid Mechanics* 616, 263-301.

Petersson, S., P. Dyverfeldt, A. Sigfridsson, J., Lantz, C. J., Carlhäll and T. Ebbers (2016). Quantification of turbulence and velocity in stenotic flow using spiral three-dimensional phase-contrast MRI. *Mag. Res. Med.* 75, 1249–1255.

Pinho, F. T., P. J. Oliveira and J. P. Miranda, (2003). Pressure losses in the laminar flow of shear-thinning power-law fluids across a sudden axisymmetric expansion. *International Journal of Heat and Fluid Flow* 24, 747–761.

Ponthieux, G. (1991). Flow of shear thinning fluids through sudden expansions. PhD Thesis, University of Henri-Poncaré Nancy-I, (1991) pp. 121. (In French)

Poole, R. J., M. A. Alves, P. J. Oliveira, and F. T. Pinho (2007). Plane sudden expansion flows of viscoelastic liquids. *Journal of Non-Newtonian Fluid Mechanics* 146, 79–91.

Poole, R. J. and M. P. Escudier (2003). Turbulent flow of a viscoelastic shear-thinning liquid through a plane sudden expansion of modest aspect ratio. *Journal of Non-Newtonian Fluid Mechanics* 112, 1–26.

Poole, R. J. and B. S. Ridley (2007). Development length requirements for fully-developed laminar pipe flow of inelastic non-Newtonian liquids. *ASME Journal of Fluids in Engineering* 129, 1281–1287.

Praveen, T. and V. Eswaran (2017). Transition to asymmetric flow in a symmetric sudden expansion: Hydrodynamics and MHD cases. *Computers and Fluids* 148, 103–120.

Ternik P. (2009). Planar sudden symmetric expansion flows and bifurcation phenomena of purely viscous shear-thinning fluids. *Journal of Non-Newtonian Fluid Mechanics* 157, 15–25.

Ternik P. (2010). New contributions on laminar flow of inelastic non-Newtonian fluid in the two-dimensional symmetric expansion: creeping and slowly moving flow conditions. *Journal of Non-Newtonian Fluid Mechanics* 165, 1400–1411.

Ternik, P., J., Marn and Z. Zunic, (2006). Non-Newtonian fluid flow through a planar symmetric expansion: shear-thickening fluids. *Journal of Non-Newtonian Fluid Mechanics* 13, 136–148.

Vanierschot, M. and E. Van den Bulck (2008). The influence of swirl on the reattachment length in an abrupt axisymmetric expansion. *International Journal of Heat and Fluid Flow* 29, 75–82.

Vétel, J., A. Garon, D. Pelletier and M. I. Farinas (2008). Asymmetry and transition to turbulence in a smooth axisymmetric constriction. *Journal of Fluid Mechanics* 607, 351-386.

Yamaguchi, H., A. Ito, M. Kuribayashi, X. R. Zhang and H. Nishiyama (2006). Basic flow characteristics in three-dimensional branching channel with sudden expansion. *European Journal of Mechanics B/Fluids* 25, 909–922.

Yamaguchi, H., A. Ito, M. Kuribayashi, X. R. Zhang and H. Nishiyama (2005). An experimented study on the flow characteristics in a three-dimensional cylindrical branching channel. *Flow Measurement and Instrumentation* 16, 241–249.

Zdanski, P. S. B. and M. Vaz Jr (2009). Three-dimensional polymer melt flow in sudden expansions: Non-isothermal flow topology. *International Journal of Heat and Mass Transfer* 52, 3585–3594.